Absolute Configuration in 4-Alkyl- and 4-Aryl-3,4-dihydro-2(1*H*)-pyrimidones: A Combined Theoretical and Experimental Investigation

Georg Uray, Petra Verdino, Ferdinand Belaj, C. Oliver Kappe, and Walter M. F. Fabian*

Institut für Chemie, Karl-Franzens Universität Graz, Heinrichstrasse 28, A-8010 Graz, Austria

walter.fabian@uni-graz.ac.at

Received May 14, 2001

Structural features (orientation of the carboxyl group, ring puckering), electronic absorption, and circular dichroism spectra of 4-alkyl- and 4-aryl-dihydropyrimidones **1**−**5** are calculated by semiempirical (AM1, INDO/S), ab initio (HF/6-31G*, CIS/6-31G*, RPA/6-31G*), and density functional theory (B3LYP/6-31G*) methods. These calculations allow an assignment of the absolute configuration by comparison of simulated and experimental CD spectra. Although the ab initio methods greatly overestimate electronic transition energies, the general appearance of the experimental CD spectra is quite nicely reproduced by these calculations. Thus, comparison of experimental with calculated CD spectra is a reliable tool for the assignment of the absolute configuration. For 4-methyl derivatives **1**, the first enantiopure DHPM examples with no additional aromatic substituent, the stereochemistry at C4 provided by the theoretical results is confirmed by X-ray structure determination of the diastereomeric salt **6**. Additional support is the consistent HPLC elution order found for all investigated DHPMs on a cellulose-derived chiral stationary phase.

Introduction

Properly functionalized 4-aryl-3,4-dihydro-2(1*H*)-pyrimidone derivatives (DHPMs) have emerged as calcium channel modulators, antihypertensive agents, α_{1a}-adrenergic antagonists, and mitotic kinesin inhibitors.[1,2] A recent pharmacological study has suggested that for DHPM calcium channel modulators the biological activity (antagonist vs agonist activity) is dependent on the absolute configuration at the stereogenic center at C4, whereby the orientation of the C4-aryl group (*R*- or *S*-configuration) acts as a molecular switch between antagonist and agonist activity.[3] Access to enantiomerically pure DHPMs with known absolute configuration is therefore a prerequisite for the development of any cardiovascular drugs of this structural type. In the past, optically pure DHPMs were obtained by resolution of the corresponding racemic carboxylic acids via diastereomeric ammonium salts, by separation of diastereomeric derivatives bearing chiral auxiliaries at N-3,[4−6] by enantioselective HPLC[7,8] and capillary electrophoresis (CE),[9,10] or via biocatalytic resolution strategies.[10−12] In many of these cases the absolute configuration of the enantiomerically pure material had to be determined by single-crystal X-ray analysis of suitable diastereomeric derivatives.[4−6,13] Recently we have reported a simple and rapid method for determining the absolute configuration in a series of 4-aryl-DHPM derivatives using circular dichroism (CD).[14] The application of this method, based on the comparison of CD data of individual enantiomers with reference samples of known absolute configuration, has proved useful for the determination of the absolute configuration in various biologically active DHPM derivatives.[11,15]

As an alternative to experimental methods, the calculation of CD spectra of chiral molecules—either by high-level quantum-chemical methods or semiempirical procedures—has become increasingly important as a means to establish absolute configuration.[16−22] Herein we report a detailed analysis of the CD spectra of 4-aryl- and

* Corresponding author: Dr. Walter M. F. Fabian, Institut für Chemie, Karl-Franzens Universität Graz, Heinrichstrasse 28, A-8010 Graz, Austria. URL: http://www-ang.uni-graz.ac.at/~fabian/

(1) Kappe, C. O. *Acc. Chem. Res.* **2000**, *33*, 879−888.
(2) Kappe, C. O. *Eur. J. Med. Chem.* **2000**, *35*, 1043−1052.
(3) Rovnyak, G. C.; Kimball, S. D.; Beyer, B.; Cucinotta, G.; DiMarco, J. D.; Gougoutas, J.; Hedberg, A.; Malley, M.; McCarthy, J. P.; Zhang, R.; Moreland, S. *J. Med. Chem.* **1995**, *38*, 119−129.
(4) Atwal, K. S.; Swanson, B. N.; Unger, S. E.; Floyd, D. M.; Moreland, S.; Hedberg, A.; O'Reilly, B. C. *J. Med. Chem.* **1991**, *34*, 806−811.
(5) Rovnyak, G. C.; Atwal, K. S.; Hedberg, A.; Kimball, S. D.; Moreland, S.; Gougoutas, J. Z.; O'Reilly, B. C.; Schwartz, J.; Malley, M. F. *J. Med. Chem.* **1992**, *35*, 3254−3263.
(6) Nagarathnam, D.; Miao, S. W.; Lagu, B.; Chiu, G.; Fang, J.; Dhar, T. G. M.; Zhang, J.; Tyagarajan, S.; Marzabadi, M. R.; Zhang, F. Q.; Wong, W. C.; Sun, W. Y.; Tian, D.; Wetzel, J. M.; Forray, C.; Chang, R. S. L.; Broten, T. P.; Ransom, R. W.; Schorn, T. W.; Chen, T. B.; O'Malley, S.; Kling, P.; Schneck, K.; Benedesky, R.; Harrell, C. M.; Vyas, K. P.; Gluchowski, C. *J. Med. Chem.* **1999**, *42*, 4764.
(7) Kleidernigg, O. P.; Kappe, C. O. *Tetrahedron: Asymmetry* **1997**, *8*, 2057−2067.
(8) Lewandowski, K.; Murer, P.; Svec, F.; Fréchet, J. M. J. *J. Comb. Chem.* **1999**, *1*, 105−112.
(9) Lecnik, O.; Schmid, M. G.; Kappe, C. O.; Gübitz, G. *Electrophoresis* **2001**, *22*, in press.
(10) Wang, F.; Loughlin, T.; Dowling, T.; Bicker, G.; Wyvratt, J. *J. Chromatogr. A* **2000**, *872*, 279−288.
(11) Schnell, B.; Strauss, U. T.; Verdino, P.; Faber, K.; Kappe, C. O. *Tetrahedron: Asymmetry* **2000**, *11*, 1449−1453.
(12) Schnell, B.; Krenn, W.; Faber, K.; Kappe, C. O. *J. Chem. Soc., Perkin Trans. 1* **2000**, 4382−4389.
(13) Kappe, C. O.; Uray, G.; Roschger, P.; Lindner, W.; Kratky, C.; Keller, W. *Tetrahedron* **1992**, *48*, 5473−5480.
(14) Krenn, W.; Verdino, P.; Uray, G.; Faber, K.; Kappe, C. O. *Chirality* **1999**, *11*, 659−662.
(15) Kappe, C. O.; Shishkin, O. V.; Uray, G.; Verdino, P. *Tetrahedron* **2000**, *56*, 1859−1862.
(16) Sandström, J. *Chirality* **2000**, *12*, 162−171.
(17) Hansen, A. E.; Bak, K. L. *Enantiomer* **1999**, *4*, 455−476.
(18) Hansen, A. E.; Bouman, T. D. *Adv. Chem. Phys.* **1980**, *44*, 545−644.

10.1021/jo010491l CCC: $20.00
Published on Web 09/01/2001

Chart 1

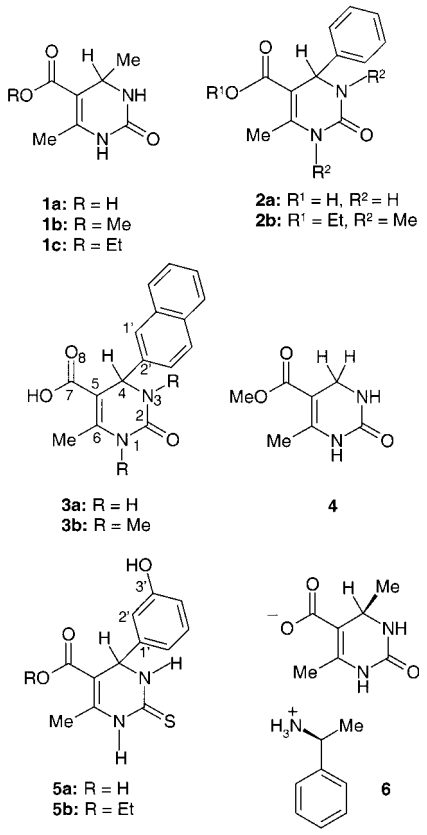

4-alkyl-DHPMs (see Chart 1 for structures) and describe computational methods that facilitate the analysis of the CD data and the assignment of absolute configuration in this series of compounds. The results obtained thereby are corroborated by X-ray structure determination of the diastereomeric derivative **6**.

Results and Discussion

Since the CD spectrum of a molecule also strongly depends on molecular conformation, for a prediction of absolute configuration by theoretical calculations, a detailed study of conformational equilibria is required.[23−25] Thus, in the following, first results of the calculations with respect to structural features of DHPMs will be presented. Second, experimental and computed UV/Vis spectra will be described. Finally, CD spectra simulated with the aid of calculated rotational strengths will be used for an assignment of the absolute configuration of the investigated compounds (see Chart 1 for structures).

Structural Features. A detailed experimental (X-ray crystallography) and computational investigation on the structure, especially ring puckering and conformational properties of the ester moiety as well as the C4 substituent, for several DHPMs, has already been published.[26,27] Therefore, in the following only salient structural features will be described: orientation of the carboxyl group (τ_1 = <(C6−C5−C7−O8), for atom numbering see Chart 1), ring puckering (height of N1 (h(N1)) and C4 (h(C4)) above C2−N3−C5−C6 plane), position (pseudoaxial vs pseudoequatorial) of the C4-substituent (τ_2 = <(C6−C5−C4−C1′); for compound **3a**, τ_2 = <(C6−C5−C4−C2′); ϕ = angle between the planes formed by C2−N3−C5−C6 and N3−C4−C5, and orientation of the aryl group (τ_3 = <(H−C4−C2′−C1′) for **3a**, τ_3 = <(H−C4−C1′−C2′) for **2a** and **5a**, Table 1).

Dihydropyrimidones adopt a pseudoboat conformation of the six-membered ring with a pseudoaxial orientation of the C4-substituent. No minimum corresponding to a pseudoequatorial arrangement of this substituent could be found. Due to the amide resonance, the dihydropyrimidine ring is extremely flattened at N1. Generally, the computations lead to a somewhat smaller ring puckering as found in the solid state by X-ray crystallography. With respect to the orientation of the carboxyl group, all computational methods predict a greater stability of the s-cis conformation irrespective of the C4-substituent (see Table 1). The energy difference between these two conformations is, however, quite small. In the solid state, intermolecular interactions, especially hydrogen bonding between the carbonyl oxygen and N1−H of a second dihydropyrimidine molecule, preferentially stabilize the s-trans orientation of the carbonyl group in esters of dihydropyrimidines, although—depending on the C4-substituent—also the s-cis conformation or even both were found by X-ray structure determination.[15,27] It is interesting to note that for the 4-phenyl derivatives **2a** and **5a** the AM1 and ab initio calculations lead to a comparable pseudoaxial orientation of the substituent (τ_2 in Table 1). In contrast, for the 4-methyl derivative **1a** AM1 calculations result in a somewhat more flattened ring than do the other methods. For comparison purposes, structural data of the C4-unsubstituted derivative **4**, which already was thoroughly investigated both experimentally as well as computationally,[26] and of the diastereomeric salt **6** are included in Table 1.

X-ray Crystal Structure of 6. The crystal structure analysis confirmed compound **6** as (1*S*,4*R*) (1-phenylethyl)ammonium 1,2,3,4-tetrahydro-4,6-dimethyl-2-oxo-5-pyrimidinecarboxylate. The absolute stereochemistry at C4 in the chiral anion (4*R*) could be determined unequivocally taking into account the known configuration of the cation (1*S*). The tetrahydro-pyrimidine ring has a boat-shaped geometry with N1 and C4 as apical atoms. All the bond lengths determined agree well with the corresponding interatomic distances found in the other 1,2,3,4-tetrahydro-6-methyl-2-oxo-5-pyrimidinecarboxylates[3,27] of the Cambridge Crystallographic Database.[28] The crystal packing is mainly determined by the 2-fold hydrogen bonds between two pyrimidone rings and those between the ammonium and carboxylate groups of

(19) Koslowski, A.; Sreerama, N.; Woody, R. W. *Circular Dichroism. Principles and Applications*, 2nd ed.; Berova, N.; Nakanishi, K.; Woody, R. W., Eds.; Wiley-VCH: New York, 2000; pp 55−95.
(20) Lightner, D. A.; Gurst, J. E. *Organic Conformational Analysis and Stereochemistry From Circular Dichroism Spectroscopy*; Wiley−VCH: New York, 2000.
(21) Grimme, S.; Peyerimhoff, S. D. *Theoretical Study of Circular Dichroism Spectra in the Vacuum Ultraviolet* In *The Role of Rydberg States in Spectroscopy and Reactivity*; Sandorfy, C., Ed.; Kluwer Academic Publishers: Dordrecht, 1999.
(22) Fleischhauer, J.; Gabriel, S.; Enders, D.; Nuhring, A.; Wollmer, A. *Z. Naturforsch.* **2000**, *55B*, 1011−1014.
(23) Dong, J.-G.; Guo, J.; Akritopoulou-Zanze, I.; Kawamura, A.; Nakanishi, K.; Berova, N. *Chirality* **1999**, *11*, 707−721.
(24) Fleischhauer, J.; Jansen, Ch.; Koslowski, A.; Raabe, G.; Schiffer, J.; Wollmer, A. *Z. Naturforsch.* **1998**, *53a*, 704−710.
(25) Bringmann, G.; Stahl, M.; Gulden, K.-P. *Tetrahedron* **1997**, *53*, 2817−2822.
(26) Fabian, W. M. F.; Semones, M. A.; Kappe, C. O. *J. Mol. Struct. (THEOCHEM)* **1998**, *432*, 219−228.
(27) Kappe, C. O.; Fabian, W. M. F.; Semones, M. A. *Tetrahedron* **1997**, *53*, 2803−2816.

Table 1. Calculated Relative Energies (Δ*E*, kcal mol^{-1}) with Respect to the Most Stable Conformer and Structural Parameters for Compounds 1a−3a, 4, and 5a

	AM1	HF/3-21G	B3LYP/3-21G	HF/6-31G*	B3LYP/6-31G*
			cis-**1a**		
τ_1	−4.2	0.2	1.5	1.0	1.4
τ_2	109.3	99.3	98.6	97.9	96.7
h(N_1)	0.038	0.096	0.101	0.123	0.121
h(C_4)	0.263	0.307	0.332	0.367	0.391
ϕ	161.1	159.0	157.4	154.8	153.2
			trans-**1a**		
Δ*E*	0.82	2.08	2.24	0.87	0.83
τ_1	176.8	−178.2	−176.3	−176.7	−176.0
τ_2	109.6	99.6	98.5	97.8	96.2
h(N_1)	0.040	0.100	0.107	0.128	0.127
h(C_4)	0.264	0.309	0.338	0.371	0.401
ϕ	161.1	158.8	156.8	154.5	152.3
1a−anion[a]		X-ray (**6**)			
τ_1	180.9	167.9			
τ_2	100.3	−93.0			
h(N_1)	0.155	0.200			
h(C_4)	0.344	0.465			
ϕ	156.1	147.3			
			cis-**2a**		
τ_1	10.5	7.1	4.0	6.1	3.6
τ_2	−105.4	−104.1	−92.0	−106.5	−104.0
τ_3	−159.7	−165.2	−134.8	179.3	−179.4
h(N_1)	0.052	0.086	0.134	0.087	0.088
h(C_4)	0.313	0.243	0.425	0.270	0.310
ϕ	157.6	163.5	150.8	161.7	159.0
			trans-**2a**[b]		
Δ*E*	0.47	1.49	1.50	0.97	0.71
τ_1	−166.5	−172.9	−177.7	−172.4	−174.9 (−166.1)[b]
τ_2	−105.5	−100.4	−94.2	−105.1	−98.9 (−102.5)
τ_3	−155.6	−152.6	−138.3	−169.4	−153.4 (168.2)
h(N_1)	0.053	0.111	0.134	0.104	0.120 (0.018)
h(C_4)	0.319	0.303	0.404	0.290	0.381 (0.319)
ϕ	157.1	159.2	152.2	160.2	153.9 (157.9)

	cis-**3aA**[c]	*cis*-**3aB**[c]	*trans*-**3aA**[c]	*trans*-**3aB**[c]	X-ray[d]
Δ*E*	0.00	0.05	0.42	0.49	
τ_1	10.8	10.1	−166.2	−166.9	30.2
τ_2	−104.7	−105.9	−105.9	−105.9	96.3
τ_3	−158.1	18.6	−154.2	23.5	19.1
h(N_1)	0.055	0.049	0.056	0.051	0.049
h(C_4)	0.320	0.306	0.325	0.315	0.335
ϕ	157.1	158.0	156.7	157.4	156.7

	cis-**4**			*trans*-**4**	
	AM1	HF/6-31G*	X-ray[e]	AM1	HF/6-31G*
Δ*E*	0.00	0.00		1.22	1.26
τ_1	0.0	−4.2	−2.2	180.0	−174.7
τ_2	−122.1	−109.1	128.1	−122.3	105.4
h(N_1)	< 0.000	0.062	0.031	< 0.000	0.083
h(C_4)	0.005	0.191	0.033	0.007	0.246
ϕ	179.6	166.8	177.7	179.5	162.9

	cis-**5aA**		*cis*-**5aB**	
	AM1	HF/3-21G*	AM1	HF/3-21G*
Δ*E*	0.03	0.00	0.00	0.46
τ_1	11.6	9.2	12.8	8.3
τ_2	−107.3	−103.9	−107.7	−104.9
τ_3	19.2	18.3	−160.5	−164.9
h(N_1)	0.061	0.084	0.063	0.080
h(C_4)	0.260	0.233	0.258	0.220
ϕ	161.6	164.3	161.8	165.2

	trans-**5aA**		*trans*-**5aB**		
	AM1	HF/3-21G*	AM1	HF/3-21G*	X-ray[f]
Δ*E*	0.11	1.73	0.43	1.77	
τ_1	−165.4	−171.6	−163.2	−171.8	169.5
τ_2	−107.8	−98.6	−107.9	−99.9	95.5
τ_3	24.9	33.9	−156.1	−149.6	−166.7
h(N_1)	0.061	0.117	0.064	0.112	0.142
h(C_4)	0.263	0.315	0.262	0.297	0.386
ϕ	161.4	158.6	161.4	159.8	153.8

[a] HF/6-31G* geometry. [b] X-ray data (in parentheses) for methyl ester of **2a**.[27] [c] AM1 geometry. [d] X-ray data for 1-phenylethylammonium salt of **3a**.[13] [e] X-ray data (in parentheses) for benzyl ester of **4**.[26] [f] X-ray data for **5b**.[15]

the counterions. Selected bond lengths and angles of **6** are collected in Table S1 of the Supporting Information.

Electronic Transition Energies. The results of semiempirical INDO/S calculations are collected in Tables S2−S6 of the Supporting Information. For each model compound **1**−**5** these calculations predict two nπ^* transitions of very low intensity ($f \leq 0.001$) but non negligible rotational strength as the longest wavelength absorption bands. The calculated positions of these two nπ^* transitions vary slightly with the geometry used (≈ 30300−32300 cm^{-1} (ab initio) and ≈26300−28600 cm^{-1} (AM1), respectively) but are essentially independent of the C4-substituent. The first $\pi\pi^*$-transition (S_3) in **1a**, **2a**, **4**, and **5a** has significant intensity ($f > 0.36$) whereas in the 2-naphthyl derivative **3a** this transition is calculated by INDO/S to be the fourth one (S_4). The position of this absorption band at about 33900 cm^{-1} (AM1 geometry) is also remarkably independent of the C4-substituent. The additional $\pi\pi^*$-transition obtained at $\nu = 31300$ cm^{-1} for **3a** has also a rather low intensity ($f < 0.007$) and can be assigned to the naphthyl L_b band (for a more detailed discussion of band assignments, see below). Experimentally, for the methyl ester **3b** the longest wavelength absorption band exhibits, contrary to the other derivatives, a partly resolved vibrational fine structure; furthermore, at the long wavelength tail a shoulder which becomes more clearly visible in apolar solvents (cyclohexane, *n*-hexane) is discernible. Thus, the long-wavelength band in the UV spectrum of **3b** closely resembles that of naphthalene itself. In contrast to the INDO/S procedure, the ab initio calculations (both RPA as well as CIS) invariably predict a $\pi\pi^*$-transition as the first absorption band (see Table 2) for **1a**−**4**. In **5a** the lone pair at sulfur is sufficiently high in energy; thus, also the ab initio calculations predict an nπ^*-transition as the longest wavelength absorption (Table 2). This theoretical result is completely in line with the experimental observation that substitution of sulfur for oxygen in carbonyl compounds substantially shifts the nπ^*-absorption to longer wavelengths.[29,30] Although not clearly visible in the UV/Vis spectra, the presence of this low-energy nπ^*-transition is confirmed by the CD spectra (see below). For **1a**, **2a**, **4**, and **5a**, the first $\pi\pi^*$-transition is calculated to have a quite significant oscillator strength (f = 0.3−0.5); in contrast, for **3a** both INDO/S as well as ab initio calculations predict this transition to be the third excited state of $\pi\pi^*$-type. Two additional long-wavelength $\pi\pi^*$-transitions of rather low intensity ($f < 0.1$) are obtained for **3a** by either computational method.

The basis set (6-31G*, 6-311++G**, aug-cc-pVDZ) and geometry (AM1, HF/3-21G, B3LYP/3-21G, HF/6-31G*, and B3LYP/6-31G*) dependence of the calculated excitation energies for **1a** is summarized in Tables S7 and S8 and the geometry dependence for **2a** in Table S9 of the Supporting Information. With respect to the geometry dependence of the calculated lowest $\pi\pi^*$ excitation energy, one finds (with Boltzmann-weighting of the contributions from s-cis and s-trans conformations) for both **1a** as well as **2a**: ν(AM1) < ν(B3LYP) < ν(HF) and ν(3-21G) < ν-(6-31G*), although the difference between 3-21G and 6-31G* results is very small. Increasing the size of the basis set slightly shifts the calculated lowest $\pi\pi^*$ transition of **1a** to longer wavelengths (with Boltzmann-weighting: $\nu = 44100$ (aug-cc-pVDZ), 44400 (6-311++G**), and 45500 (6-31G*) cm^{-1}, respectively). The position of the first $\pi\pi^*$ transition of the dihydropyrimidones **1**−**5** calculated by the INDO/S procedure (see Tables S2−S6 of the Supporting Information) is in very good agreement with the corresponding experimental values (see Table 3 for experimental transition energies). In contrast, ab initio calculations greatly (>10000 cm^{-1}) overestimate

Table 2. Ab Initio (RPA/6-31G* and CIS/6-31G*) Calculated Transition Energies ν (cm^{-1}), Oscillator Strengths f, and RPA/6-31G* Rotational Strengths R (10^{-40} esu^2 cm^2) for (*S*)-1a, (*S*)-1a-Carboxylate Anion, (*R*)-2a, (*R*)-3a, 4, and (*R*)-5a[a]

	RPA			CIS	
	ν	f	R	ν	f
cis-**1a**	48433	0.311	−16.948	50629	0.411
	54715	0.003	−3.077	55974	0.005
	62294	0.001	−7.307	63464	0.001
	70629	0.176	13.370	71872	0.229
trans-**1a**	48660	0.352	8.400	50884	0.467
	55037	0.003	−22.748	56368	0.005
	62379	0.001	−7.076	63544	0.001
	69843	0.190	−15.123	71027	0.252
1a-anion	53132	0.287	24.390	54676	0.006
	53756	0.007	8.338	55446	0.341
	55982	0.007	−24.958	57076	0.028
	65250	0.080	1.817	67070	0.091
cis-**2a**	47853	0.280	−143.621	49963	0.351
	49032	0.005	−3.335	50706	0.028
	49584	0.050	41.271	52085	0.043
	54813	0.000	−0.718	56068	0.000
trans-**2a**	47820	0.297	−160.432	49983	0.395
	48985	0.002	0.237	50622	0.008
	49585	0.059	28.042	52071	0.053
	54988	0.001	14.166	56308	0.002
cis-**3aA**	39254	0.034	−1.040	41936	0.029
	41564	0.001	−0.857	43283	0.002
	44911	0.355	−215.350	47029	0.462
	50331	0.001	4.387	51609	0.000
cis-**3aB**	39581	0.089	0.218	42274	0.098
	41624	0.000	−0.153	43331	0.000
	45001	0.346	−188.431	47103	0.456
	50370	0.000	0.873	51649	0.000
trans-**3aA**	39379	0.035	12.389	42056	0.030
	41606	0.002	−0.968	43322	0.003
	44994	0.405	−257.871	47111	0.527
	51115	0.002	8.883	52427	0.001
trans-**3aB**	39467	0.082	−10.034	42167	0.088
	41588	0.001	−0.381	43297	0.001
	45109	0.402	−192.831	47214	0.534
	50957	0.013	35.657	52252	0.008
cis-**4**	48263	0.353		50395	0.445
	54708	0.002		55971	0.004
	62662	0.000		63817	0.001
	71188	0.229		72527	0.312
trans-**4**	48505	0.368		50674	0.477
	54886	0.002		56214	0.002
	62636	0.000		63789	0.001
	70412	0.229		71722	0.316
cis-**5aA**	41935	0.007	25.700	42374	0.005
	44653	0.474	−229.236	46215	0.650
	47877	0.057	58.343	49637	0.058
	49262	0.026	27.439	51056	0.079
cis-**5aB**	41833	0.007	24.843	42272	0.004
	44630	0.496	−212.127	46188	0.675
	47619	0.064	0.262	49443	0.062
	49116	0.028	45.993	50908	0.066
trans-**5aA**	42007	0.011	29.720	42456	0.008
	45170	0.470	−237.333	46747	0.658
	47931	0.050	43.497	49701	0.051
	49500	0.005	25.584	51357	0.076
trans-**5aB**	41834	0.011	29.278	42284	0.008
	45001	0.498	−247.467	46574	0.688
	47787	0.041	12.676	49591	0.038
	49354	0.035	67.415	51151	0.073

[a] HF/6-31G* geometry for **1a**, its carboxylate anion, **2a** and **4**; AM1 geometry for **3a**, and HF/3-21G(*) geometry for **5a**.

(28) Allen, F. H.; Kennard, O. *Chem. Des. Autom. News* **1993**, *8*, 31−37.
(29) Maciejewski, A.; Steer, R. P. *Chem. Rev.* **1993**, *93*, 67.
(30) Milewska, M. J.; Gdaniec, M.; Polonski, T. *J. Org. Chem.* **1997**, *62*, 1860−1862.

Table 3. Experimental UV Data of DHPMs in EtOH

compound	ν/cm^{-1}	ϵ
1a	35800	9500
1b	35500	10700
	(35300)[a]	
	(49000)[a]	
2b	33800	8400
	43900	8600
3b	34800	9700
	36000	9700
	45000	67100
4	34800	8800
	(34700)[a]	
	47200	7500
	(48300)[a]	
5b	32700	13200

[a] In aqueous solution.

this excitation energy. The naphthyl derivatives **3** show an intense second band at about 45500 cm^{-1}, e.g., **3b** (EtOH): ν = 45000 cm^{-1}, ϵ = 67100, see Table 3). For the phenyl derivatives **2**, this band extends above 50000 cm^{-1}; however, depending on the experimental conditions, a more or less clearly resolved shoulder (or even separate maximum) is discernible with ν = 43900 cm^{-1}, ϵ = 8600. For the methyl derivative **1b** as well as the C4-unsubstituted compound **4**, a hypsochromic shift of this band to ν = 49000 cm^{-1} (**1b**) and to ν = 48300 cm^{-1} (**4**) in aqueous solution can be observed (see Table 3). Ab initio CIS/6-31G* and RPA/6-31G* calculations (see Table 2) also predict a second rather intense transition at ≈21000 cm^{-1} (**1a**)), ≈24000 cm^{-1} (**2a**), and ≈9000 cm^{-1} (**3a**), above the first (second in **3a**) $\pi\pi$*-transition, respectively. The corresponding experimental values are: 13700 cm^{-1} (**1b**), 13600 cm^{-1} (**4**); 10100 cm^{-1} (**2b**), and ≈10000 cm^{-1} (**3b**). The carboxylic acid **1a** shows a pH-dependent UV spectrum: in acidified aqueous solution the spectrum is essentially identical to those of the esters **1b** and **1c**. In aqueous alkali (pH > 8.5), where carboxylate **1a**$^-$ is predominant, the first absorption band is blue shifted by ≈2000 cm^{-1}. CIS/6-31G* calculations yield a shift of ≈5000 cm^{-1} (Table 2).

Rotational Strengths. Ab initio calculated rotational strengths for (*S*)-**1a**, (*R*)-**2a** (HF/6-31G* geometry) as well as (*R*)-**3a** (AM1 geometry) and (*R*)-**5a** (HF/3-21G* geometry) are summarized in Table 2, INDO/S results as well as basis set and geometry dependencies are collected in Tables S2−S9 of the Supporting Information. The experimental UV and CD spectra of (*S*)-**1a**, (*S*)-**1b** and the anion of (*S*)-**1a** are shown in Figure 1. It can be clearly seen that replacing the ester group by carboxyl in the model systems used for the calculations will have no discernible effect on the simulated CD spectra. The simulated spectra of (*S*)-**1a** using different basis sets (see below) are quite similar. Therefore, the calculated RPA/6-31G* results for **2a**, **3a**, and **5a**, where calculations using larger basis sets are impracticable, should be of sufficient reliability.

On the other hand, since it is well-known that INDO/S-type calculations of electronic excitation energies greatly underestimate those of nπ*-transitions,[31] a comparison of CD spectra simulated on the basis of INDO/S-derived rotational strengths with experimental ones is hardly possible for compounds where such transitions are expected to be in the region of $\pi\pi$*-transitions. In fact, for

(31) Becker, R. S.; Chakravorti, S.; Gartner, C. A.; de Graca Miguel, M. *J. Chem. Soc., Faraday Trans.* **1993**, *89*, 1007−1019.

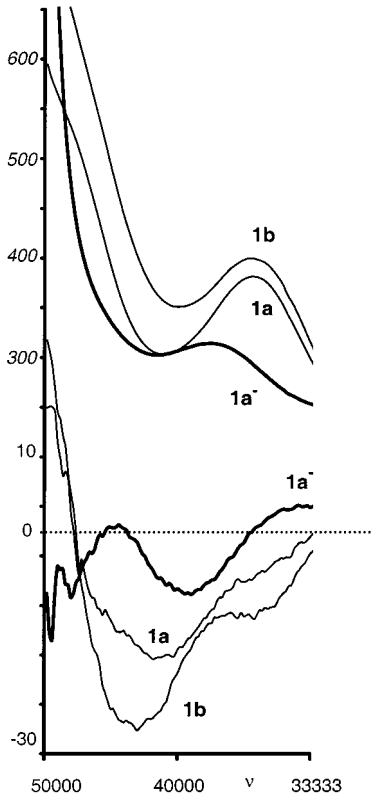

Figure 1. Experimental UV and CD spectra of acid (*S*)-**1a**, its anion (*S*)-**1a**$^-$, and methyl ester (*S*)-**1b**.

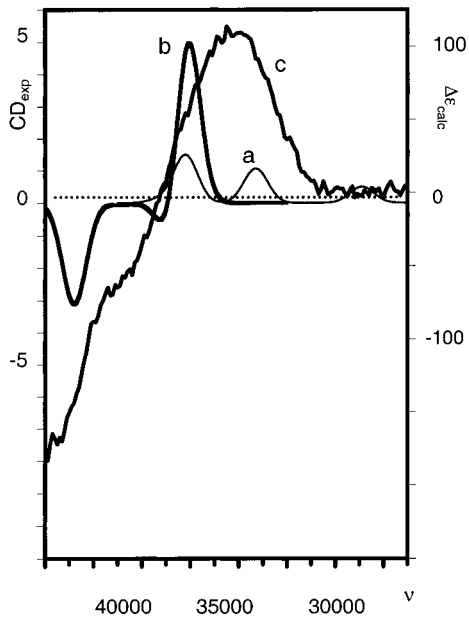

Figure 2. Simulated[48] (INDO/S (a) and RPA/6-31G* (b), HF/6-31G* geometry) and experimental (**c**) CD spectra of (*S*)-**2a**. The spectrum simulated on the basis of RPA/6-31G* rotational strengths is red shifted by 16000 cm^{-1}.

2a INDO/S predicts the two nπ*-transitions to lie 3400 cm^{-1} and 7500 cm^{-1}, respectively, below the first $\pi\pi$*-transition (see Figure 2a). In contrast, ab initio CIS/6-31G* calculations predict these same two transitions to be 6000 and 13400 cm^{-1}, respectively, above the first $\pi\pi$*-transition. Although the calculated oscillator strengths of these nπ*-transitions are very small, the respective rotational strengths are by no means negligible (see

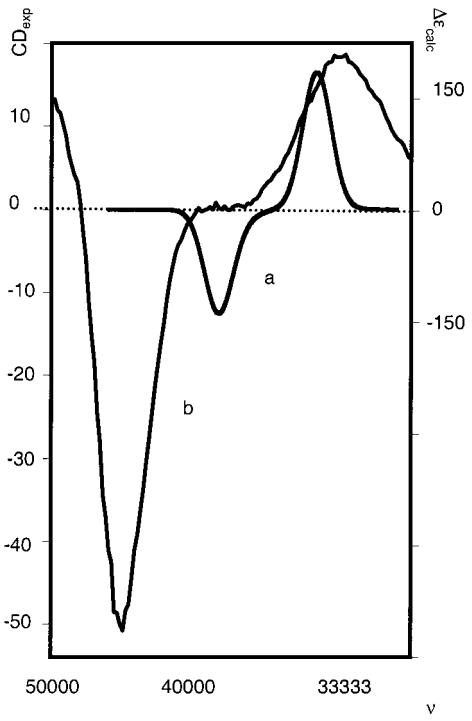

Figure 3. Comparison of the simulated[48] (RPA/6-31G*, AM1 geometry) CD spectrum for (*S*)-**3a** (a) with the experimental CD spectrum of (*S*)-**3b** (b). The simulated spectrum is red shifted by 16000 cm^{-1}.

Figure 2 for a comparison of the simulated CD spectra of **2a** with the experimental one). It should be noted that the third band in Figure 2a corresponds to the first one in Figure 2b. Obviously, then, for compounds with nπ*-transitions possibly lying in the vicinity of $\pi\pi$*-transitions, simulated CD spectra resulting from INDO/S-type calculations might be unreliable. Thus, in the following only results for rotational strengths obtained by ab initio RPA calculations will be discussed.

The experimental CD spectra of the (*S*)-enantiomers of 4-aryl-DHPMs, e.g., **2b** (Figure 2c) and **3b** (Figure 3b), show a positive sign of the first and a negative sign for the second band.[14] However, whereas for derivatives of **2** substituted in the phenyl ring, e.g., 3-nitrophenyl- or 2,3-dichlorophenyl-DHPM as well as for **3b**, this second CD band corresponds to a well-defined maximum, for **2b** no such clear maximum below 50000 cm^{-1} is discernible.[14] In the case of (*R*)-**5b** in addition to this *minus*−*plus* couplet a weak positive Cotton effect, attributable to the presence of the thiocarbonyl nπ*-transition, at ≈29400 cm^{-1} can be seen.[15] Simulated CD spectra are at least in qualitative agreement with these experimental findings (Figure 2, Figure 3 and Figure S1 of the Supporting Information). As already pointed out in the previous section, the energies of the calculated electronic transitions are grossly overestimated and, consequently, the positions of the respective CD bands appear at wavelengths that are considerably too short.

Despite the similarity between the UV spectra of 4-methyl-DHPMs **1** and those of 4-aryl derivatives **2**, **3**, and **5**, compounds of type **1** show completely different CD spectra. The most notable features are the presence of two bands of like sign with the second one at a position (ν = 41700 cm^{-1}) where no corresponding absorption in the UV spectrum is present. Thus, no assignment of the absolute configuration of this DHPM derivative on the basis of the previously described experimental[14] method is possible. Given the computational results described above, it was expected that comparison between experimental CD spectra and those simulated on the basis of calculated rotational strengths would be helpful for the correct assignment of absolute configuration for 4-alkyl derivatives **1**.

Surprisingly, whereas for **2a** and **5a**, RPA/6-31G* calculations predict a negative sign of the first band in the CD spectrum of the molecule with (*R*)-configuration regardless of whether ab initio, B3LYP or semiempirical AM1 molecular geometries are used, the simulated CD spectrum of compound **1a** shows a distinct dependence on the input structure: using the AM1 geometry for the (*S*)-enantiomer of **1a**, a *plus*−*minus* couplet for the two first transitions is predicted; in complete contrast, using an ab initio or density functional (B3LYP) geometry, for these very same transitions a *minus*−*minus* couplet is obtained (see Figure 4). This contrasting result is independent of the basis set used in the calculations.

A possible explanation for the above discrepancy might be provided by the fact that the ab initio calculations on **1a** lead to an orientation of the C4-methyl group more closely resembling an axial arrangement than do the AM1 calculations. For instance, the torsional angle τ_2 is ≈10° smaller for ab initio geometries (see Table 1). In contrast, for compound **2a**, there is essentially (except for the B3LYP/3-21G geometry) no difference between the AM1 and ab initio values of τ_2 (Table 1). Recently, experimental precedence for the fact that even a rather small structural change can lead to an almost mirror image CD spectrum[16,32] was found: (*S*)-**7** and (*R*)-**8** exhibit CD spectra which appear as mirror images; however, because of substituent priorities, both compounds have a similar spatial arrangement of the substituents in the two enantiomers.

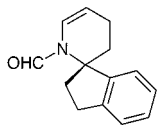

7

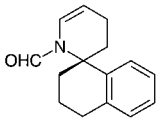

8

Furthermore, the potential energy function for changing τ_2 is in the vicinity of the minimum quite flat, e.g., decreasing the AM1 value of τ_2 (≈110°) in the AM1 geometry of **1a** by ≈10° to that obtained by HF/6-31G* calculations leads only to an energy increase of = 0.8 kcal mol^{-1}. Similarly, increasing the HF/6-31G* value of τ_2 (≈98°) in the ab initio geometry by the same amount also leads to a rather small increase of the total energy (= 0.5 kcal mol^{-1}). RPA/6-31G* calculations of rotational strengths, using an AM1 geometry with such a decreased value of τ_2 but otherwise completely optimized, indeed result in simulated CD spectra that closely resemble those obtained when ab initio geometries were used. Obviously then, the amount of puckering in **1** plays a significant role for the chiroptical properties of 4-methyl-DHPM. Inclusion of conformations up to an energy range of 3 kcal mol^{-1} has been recommended for exciton chirality CD calculations of steroidal naphthoates by semiempirical methods.[23]

(32) Ripa, L.; Hallberg, A.; Sandström, J. *J. Am. Chem. Soc.* **1997**, *119*, 5701−5705.

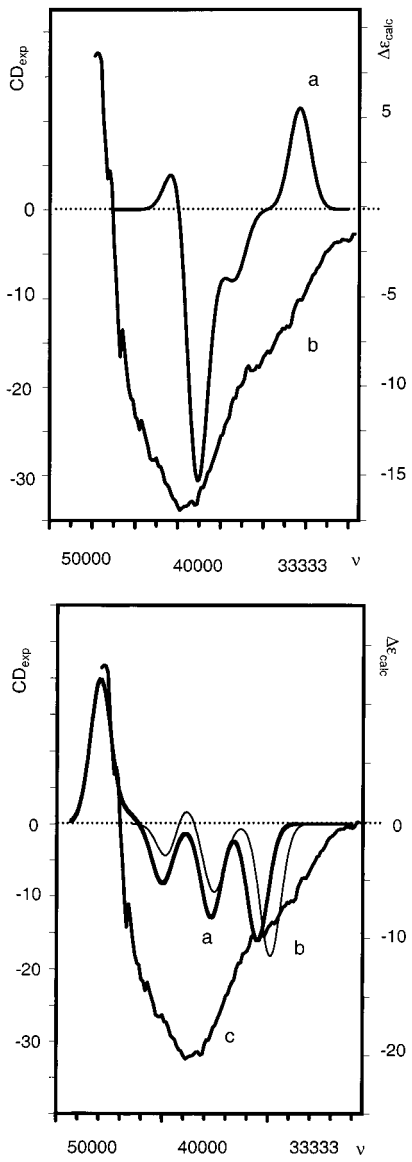

Figure 4. Comparison of the simulated[48] (RPA/aug-cc-pVDZ, AM1 geometry, (a)) CD spectrum for (*S*)-**1a** with the experimental one (b, upper part) and those simulated using HF/6-31G* geometries (RPA/6-31G* (a), RPA/aug-cc-pVDZ (b) with the experimental one (c, lower part). The simulated spectra are red shifted by 16000 cm^{-1}.

To unambiguously establish the absolute configuration of 4-alkyl derivatives **1**, a X-ray structure determination of the diastereomeric salt **6** was performed. Thereby the CD spectrum showing two negative bands can be assigned to the (*S*)-enantiomer in complete agreement with the calculations based on ab initio geometries for **1a**.

Nature of Electronic States. The main configurations obtained by ab initio CIS/6-31G* calculations for the first few electronically excited states are collected in Table S10 of the Supporting Information. For compound **1a** the first electronic transition is dominated by the HOMO → LUMO singly excited configuration which can be viewed as a transition mainly involving the enamine moiety of **1a** (see Figure 5). The second and third transition are found to be of the nπ*-type, whereas S_4 is a $\pi\pi$*-state as also indicated by its relatively large calculated oscillator strength (Table 2). This transition can be assigned to the second band observable at about 47600 cm^{-1} in the experimental UV spectra of **1a**, **1b**, and **4**. On the basis of the orbital characteristics, it represents an intramolecular charge transfer with the O=C2−N3−C4 amide moiety as donor and the enamine part of the heterocycle as acceptor.

The rotational strengths for S_4 are calculated to have opposite signs depending on the conformation of the carboxyl group (see Table 2) in **1a**. Thus, on Boltzmann-averaging over the two conformations, the associated bands in the CD spectrum should approximately cancel each other. In contrast, despite the low oscillator strength of S_3, the corresponding rotational strengths are of the same sign for both conformers and, thus, on Boltzmann-averaging add up. Therefore, in agreement with the experimental observations, in 4-alkyl-DHPMs of type **1**, in the CD spectrum a band at a wavelength where no electronic absorption can be seen should appear.

The first excited state of **2a** is calculated to be a mixture of the HOMO → LUMO and HOMO-2 → LUMO configuration. All three orbitals involved show considerable delocalization between the enamine substructure of the dihydropyrimidone moiety and the phenyl ring (see Figure 6). Therefore, a clear-cut interpretation of this transition in terms of localized excitations is not strictly possible. However, both configurations involve a bonding → antibonding transition of the enamine moiety similar to that seen in **1a**. In addition, the HOMO → LUMO transition also shows characteristics of the benzene L_a band. The L_a transition of aromatic groups, e.g., benzoates, is frequently used for the determination of the absolute configuration of bichromophoric chiral molecules by the exciton chirality method.[33] For instance, in this connection it should be noted that the interaction of the benzene L_a band of the phenyl group with that of the benzoyl moiety in benzoates of α-aryl-substituted alcohols was proposed to be responsible for their CD spectra.[34] It is tempting to interpret the circular dichroism spectra of C4-aryl-substituted dihydropyrimidones in an analogous manner: The first electronic transition in **1a** is calculated to be polarized in the dihydropyrimidine plane approximately perpendicular to the C5−C6 bond. Consequently, exciton coupling between this band and the phenyl L_a transition will lead to a negative first Cotton effect in (*R*)-**2** (negative chirality of the two transition moments) as found experimentally.

The second and third transition are almost exclusively localized within the benzene ring whereas S_4 and S_5 (CIS/6-31G*) or S_6 (RPA) are of the nπ^* type. Finally, the second electronic transition with a substantial oscillator strength ($f \approx 0.9$, see Table 2), i.e., S_5 (RPA) or S_6(CIS) corresponds to the B_a-type band of aromatic hydrocarbons with substantial or even equal admixture of the bonding → antibonding transition of the enamine moiety as also characteristic for S_1. The second band of opposite sign to the first one in the CD spectrum of **2b** (see Figure 2) can be attributed to this latter electronic transition. According to the ab initio calculations, the first two transitions in **3a** have rather low intensities. They can be assigned as L_a and L_b naphthalene bands, respectively, with some intramolecular charge transfer from the naphthalene toward the heterocyclic moiety (the NHOMO (orbital no. 73) and HOMO (orbital no. 74, Table S10 of the Sup-

(33) Harada, N.; Nakanishi, K. *Circular Dichroic Spectroscopy. Exciton Coupling in Organic Stereochemistry;* University Science Books: Mill Valley, 1983.

(34) Adam, W.; Lukacs, Z.; Viebach, K.; Humpf, H.-U.; Saha-Möller, C. R.; Schreier, P. *J. Org. Chem.* **2000**, *65*, 186−190.

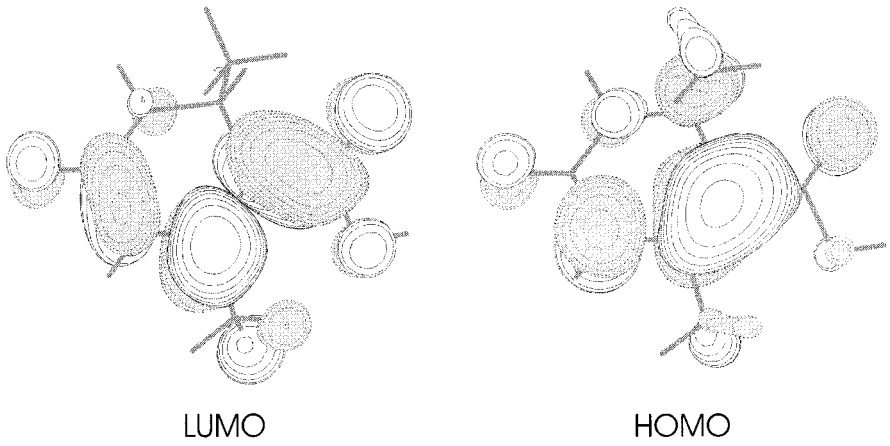

Figure 5. Plots[50] of HOMO and LUMO (HF/6-31G*//HF/6-31G*) of s-trans-**1a**.

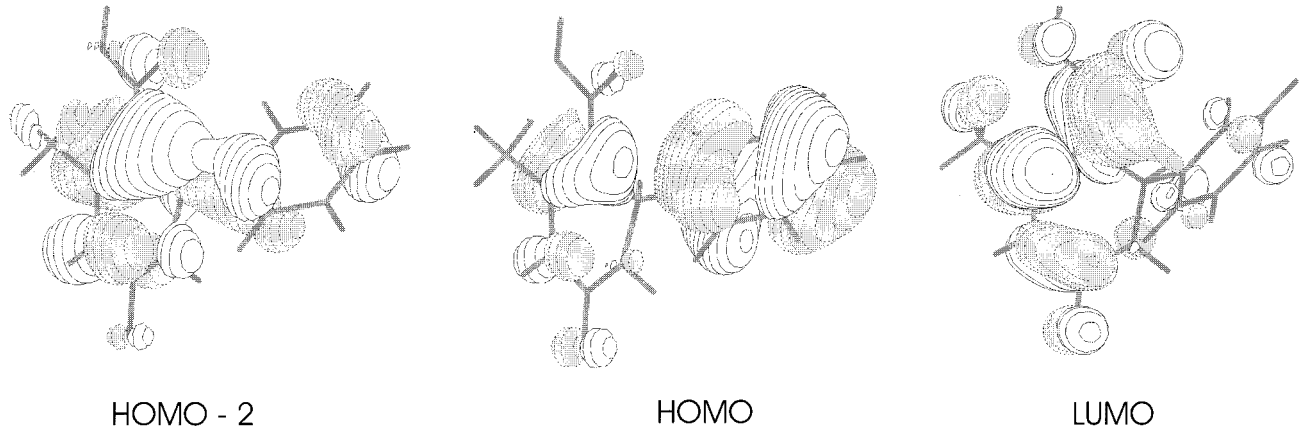

Figure 6. Plots[50] of HOMO-2, HOMO, and LUMO of s-trans-**2a** (HF/6-31G*, AM1 geometry).

porting Information) are almost exclusively localized at the naphthalene ring, whereas the LUMO (orbital no. 75) and NLUMO (orbital no. 76) are delocalized over the whole molecule but have also the characteristic features of the naphthalene LUMO). The third excited singlet state in **3a** corresponds to S_1 of both **1a** and **2a.** It can be assigned to a transition mainly localized within the enamine subunit with some charge-transfer toward the naphthalene ring (see Figure S2 of the Supporting Information). The large positive CD band seen in **3** results from S_5 and/or S_6 (see Table 2 and Table S10 of the Supporting Information). Both transitions involve the same molecular orbitals as are in S_1 and S_2, i.e., can be described as naphthalene $B_{a,b}$ bands with charge transfer from the naphthalene ring toward the dihydropyrimidone.

In **5a** the CD band at the longest wavelength can be associated with the thiocarbonyl nπ^* transition. Otherwise the various electronic transitions closely resemble those of **2a** and/or **3a**.

Conclusions

Theoretical calculations of rotational strengths by the semiempirical INDO/S or the ab initio RPA procedure for aryl and alkyl C-4-substituted dihydropyrimidones have been described and correlated with experimental data. CD spectra simulated using INDO/S results are less reliable because of the underestimation of the nπ^*-excitation energies. On the other hand, the positions of $\pi\pi^*$-transitions calculated by INDO/S are in excellent agreement with experimental UV spectra. Ab initio RPA and CIS calculations greatly overestimate transition energies. For 4-aryl derivatives, results based either on ab initio (HF/6-31G*) or density functional theory (B3LYP/6-31G*) geometries are quite similar to those obtained using semiempirical AM1 geometries. In sharp contrast, for 4-methyl-DHPM **1a**, the geometry used (AM1 vs ab initio) significantly influences the appearance of the simulated CD spectra. Only those based on ab initio structures lead to simulated spectra in agreement with experimental findings. Whereas the CD spectra of 4-aryl DHPMs are characterized by two maxima with a positive long wavelength and a negative short wavelength $\Delta\epsilon$ for the (*S*)-enantiomers ((*R*)-enantiomer for 4-(2,3-dichlorphenyl)-DHPM because of the CIP priorities), in case of 4-alkyl derivatives two bands with like sign are found. The second one of these two bands corresponds to a dipole-forbidden electronic transition. Simulated CD spectra based on ab initio geometries of **1a** and rotational strengths calculated by the ab initio RPA method, apart from a shift toward shorter wavelengths, show good agreement with the experimental spectra. The assignment of the absolute configuration of 4-alkyl-DHPM **1** on the basis of a comparison between experimental and calculated CD spectra was further confirmed by a X-ray structure determination of diastereomeric salt **6**. The first electronic transition of all DHPMs studied can be associated with the enamine chromophore. In the case of 4-aryl

derivatives a substantial delocalization between the aromatic moiety and the enamine subunit is evident from the spatial characteristics of the orbitals involved in the respective electronic transitions.

Experimental Section

Liquid Chromatography with Chiral Stationary Phases. 1,3,5-Tri-*tert*-butylbenzene was used as void volume marker. Solvents (*n*-heptane, 2-propanol) were of HPLC-grade. Columns and conditions used: DAICEL Chiralcel ODH (250 × 4.6 mm) for enantioseparation of methyl ester **1b** and ethyl ester **1c**; mobile phase: *n*-heptane/2-propanol 90/10; flow 1.0 mL/min; 25 °C; **1b**: $k'_1 = 2.23$, $\alpha = 1.17$, res = 1.13; **1c**: $k'_1 = 1.90$, $\alpha = 1.25$; res = 1.85; first eluted enantiomer (*S*). Enantiomeric purity of acid **1a** could be analyzed without derivatization using normal phase conditions and a 125 × 4.6 mm ULMO-column (REGIS, Morton Groove, Il, USA); mobile phase: *n*-heptane/2-propanol 94/6 and 0.1% trifluoroacetic acid/0.1% diisopropylamine; flow 1 mL/min; 25 °C; **1a**: $k'_1 = 6.62$, $\alpha = 1.10$, res = 0.60; first eluted enantiomer (*S*) on the (*R,R*)-ULMO. Resolution was good enough for checking diastereomeric purity of phenylethylamine salt **6**. However, conversion of acid **1a** to baseline-separated methyl ester **1b** was accomplished after addition of excess diazomethane in ether to a suspension of the acid or the acidified salt (HCl) in methanol. Elution order was established after X-ray analysis of diastereomeric pure salt **6.**

Formation and Separation of Diastereomeric Salt 6. A sample (170 mg, 1.00 mmol) of the racemic acid **1a** was suspended in analytical grade methanol (15 mL). To this solution was added *(S)*-phenylethylamine (133 mg, 1.10 mmol). After being stirred for 30 min, the slightly turbid solution was filtered and the solvent was slowly evaporated to a volume of about 1 mL. After several trials yielding very small crystals containing both diastereomers in exactly equal amounts, clear crystals (60 mg, 21%) could be isolated with a diastereomeric excess of 77%. Recrystallization using the same method at room temperature yielded 45 mg crystals 88% de, and two further purification steps yielded a diastereomer de of >99% containing the (*R*)- acid (*S*)-phenylethylamine salt as revealed by X-ray analysis.

Calorimetric Data of 6. The differential scanning calorimetry plots were recorded between 25 and 300 °C with a heating rate of 5 °C/min and about 1 mg compound in sealed aluminum crucibles (11 bar). Calorimetric data of diastereomeric mixture **6**: mp onset 135.9 °C, first peak maximum 142.7 °C, $\Delta H = 3.9$ mcal/mg, second mp onset at 152.3 °C, peak maximum 161.3 °C, $\Delta H = 8.4$ mcal/mg. Calorimetric data of pure diastereomer **6**: mp onset 185.2 °C, peak maximum 189 °C, $\Delta H = 5.5$ mcal/mg.

X-ray Diffraction Analysis of DHPM Salt 6. All the measurements were performed using graphite-monochromatized Mo Kα radiation at 90 K: $C_{15}H_{21}N_3O_3$, M_r 291.35, monoclinic, space group $P2_1$, $a = 7.953(3)$ Å, $b = 7.196(4)$ Å, $c = 12.664(4)$ Å, $\beta = 94.84(3)°$, $V = 722.2(4)$ Å^3, $Z = 2$, $d_{calcd} = 1.340$ g cm^{-3}, $\mu = 0.095$ mm^{-1}. A total of 3899 reflections were collected ($\Theta_{max} = 30°$), from which 2999 were unique ($R_{int} = 0.0319$), with 2833 having $I > 2\sigma(I)$. The structure was solved by direct methods (SHELXS-97)[35] and refined by full-matrix least-squares techniques against F^2 (SHELXL-97).[36] The non-hydrogen atoms were refined with anisotropic displacement parameters. The H-atoms were refined with common isotropic displacement parameters for the H-atoms of the same methyl group and idealized geometry with C−H distances of 0.98 Å. For 205 parameters final *R* indices of $R = 0.0393$ and $wR^2 = 0.1010$ (GOF = 1.024) were obtained. The largest peak in a difference Fourier map was 0.321eÅ^{-3}. Additional details are provided in Tables S11−S16 and Figure S3 (ORTEP plot[37] of the Supporting Information). The crystal structure of **6** has been deposited at the Cambridge Crystallographic Data Centre and allocated the deposition number CCDC 162128.

UV and CD Spectroscopy. UV-spectra were recorded at ambient temperature using 1 cm rectangular quartz cells. Solvents of spectroscopic quality were used, sample concentration about 3×10^{-5} mol/L. In water the full carboxylate form of **1a** was generated by adjusting the pH to about 8 with ammonia, the undissociated carboxylic acid by adjusting the pH to about 2 with sulfuric acid. CD measurements were carried out using a 0.1 cm path length cell with a volume of 350 μL at 20 °C with methanol as solvent. Spectra were recorded between 400 and 190 nm with 1 nm resolution at a scan speed of 100 nm/min and resulted from averaging three scans. The final spectra were baseline-corrected by subtracting the corresponding methanol spectrum obtained under identical conditions. Results were expressed as CD [mdeg] and UV [a.u.] at the given wavelengths.

Computational Details. Geometries were optimized by the semiempirical AM1 method[38] using the VAMP program package[39] as well as by ab initio Hartree−Fock (HF) and density functional theory (B3LYP)[40,41] calculations using the Gaussian 98 program suite.[42] For geometry optimizations, the 3-21G and 6-31G* basis sets were used. Electronic circular dichroism spectra were calculated by the semiempirical DZDO program[43] using Zerner's spectroscopic parameters[44] as well as by ab initio methods using the random phase approximation (RPA)[17] as implemented in the Dalton program.[45] Basis sets used for these calculations were of 6-31G*, 6-311++G**, and aug-cc-pVDZ[46] quality. Both the dipole length as well as velocity formulation of *f* and *R* were used. The differences between these two formulations are found to be negligible and, thus, in the tables only the results obtained by the dipole velocity formulation are given. Ab initio calculations of electronic excitation energies were also done by the single excitation configuration interaction (CIS) procedure (Gaussian 98). CD spectra were simulated[24,47−49] as sums of Gaussians centered at the wavelengths of the corresponding electronic transitions and multiplied by the calculated rotational strength. An empirical half bandwidth of 7 nm at 1/e of the maximum[24,49]

(35) Sheldrick, G. M. *Program for the Solution of Crystal Structures* [SHELXS-97]. University of Göttingen, Germany, 1997.

(36) Sheldrick, G. M. *Program for the Refinement of Crystal Structures* [SHELXL-97]. University of Göttingen, Germany, 1997.

(37) Johnson, C. K. [ORTEP]. Oak Ridge National Laboratory: Tennessee, 1965.

(38) Dewar, M. J. S.; Zoebisch, E. G.; Healy, E. F.; Stewart, J. J. P. *J. Am. Chem. Soc.* **1985**, *107*, 3902−3909.

(39) Clark, T. *VAMP 4.4, Erlangen Vectorized Molecular Orbital Package*, Computer-Chemie-Centrum, University Erlangen-Nürnberg, Germany, 1992.

(40) Becke, A. D. *J. Chem. Phys.* **1993**, *98*, 5648−5642.

(41) Lee, C.; Yang, W.; Parr, R. G. *Phys. Rev. B* **1988**, *37*, 785−789.

(42) Gaussian 98, R. A. 3.; Frisch, M. J.; Trucks, G. W.; Schlegel, H. B.; Scuseria, G. E.; Robb, M. A.; Cheeseman, J. R.; Zakrzewski, V. G.; Montgomery, Jr. J. A.; Stratmann, R. E.; Burant, J. C.; Dapprich, S.; Millam, J. M.; Daniels, A. D.; Kudin, K. N.; Strain, M. C.; Farkas, O.; Tomasi, J.; Barone, V.; Cossi, M.; Cammi, R.; Mennucci, B.; Pomelli, C.; Adamo, C.; Clifford, S.; Ochterski, J.; Petersson, G. A.; Ayala, P. Y.; Cui, Q.; Morokuma, K.; Malick, D. K.; Rabuck, A. D.; Raghavachari, K.; Foresman, J. B.; Cioslowski, J.; Ortiz, J. V.; Stefanov, B. B.; Liu, G.; Liashenko, A.; Piskorz, P.; Komaromi, I.; Gomperts, R.; Martin, R. L.; Fox, D. J.; Keith, T.; Al-Laham, M. A.; Peng, C. Y.; Nanayakkara, A.; Gonzalez, C.; Challacombe, M.; Gill, P. M. W.; Johnson, B.; Chen, W.; Wong, M. W.; Andres, J. L.; Gonzalez, C.; Head-Gordon, M.; Replogle, E. S.; Pople, J. A. Gaussian, Inc., Pittsburgh, PA, 1998.

(43) Downing, J.; Michl, J. *Program DZDO, Version 4.021*, University of Colorado at Boulder.

(44) Ridley, J.; Zerner, M. C. *Theor. Chim. Acta* **1973**, *32*, 111−134.

(45) Helgaker, T.; Jensen, H. J. Aa.; Joergensen, P.; Olsen, J.; Ruud, K.; Aagren, H.; Andersen, T.; Bak, K. L.; Bakken, V.; Christiansen, O.; Dahle, P.; Dalskov, E. K.; Enevoldsen, T.; Fernandez, B.; Heiberg, H.; Hettema, H.; Jonsson, D.; Kirpekar, S.; Kobayashi, R.; Koch, H.; Mikkelsen, K. V.; Norman, P.; Packer, M. J.; Saue, T.; Taylor, P. R.; Vahtras, O. *Dalton Release 1.0 1997, an Electronic Structure Program*.

(46) Dunning, T. H. *J. Chem. Phys.* **1989**, *90*, 1007−1023.

(47) Fleischhauer, J.; Koslowski, A.; Repges, Ch.; Gulden, K.-P.; Bringmann, G. *Z. Naturforsch.* **1998**, *53a*, 993−996.

(48) *Program SHAPE* was kindly provided by Prof. Dr. J. Fleischhauer, RWTH Aachen, Germany.

(49) Fleischhauer, J.; Raabe, G.; Santos, A. G.; Schiffer, J.; Wollmer, A. *Z. Naturforsch.* **1998**, *53a*, 896−902.

was used, and Boltzmann-averaging over the individual conformers was done. The effect of using constant vs variable half bandwidths on simulated CD spectra is shown in Figure S4 of the Supporting Information. Molecular orbital drawings were generated by the MOLDEN program.[50]

Acknowledgment. Part of this work was supported by the Austrian Science Fund (FWF, Project P-11994-CHE).

(50) Schaftenaar, G.; Noordik, J. H. *J. Comput.-Aided Mol. Des.* **2000**, *14*, 123−134.

Supporting Information Available: Tables of geometry and basis set dependence of calculated excitation energies, oscillator and rotational strengths (INDO/S, RPA, CIS) for **1a**−**3a**, **4**, and **5a**, details of X-ray structure determination of diastereomeric salt **6**, Cartesian coordinates of calculated structures, figures showing a comparison of simulated CD spectrum of **5a** with experimental CD spectrum of **5b**, orbital plots for **3a**, and ORTEP plot of **6**. This material is available free of charge via the Internet at http://pubs.acs.org.

JO010491L